PII: S0032-3861(96)00684-2

Polymer Vol. 38 No. 7, pp. 1521–1535, 1997

0032-3861/97/$17.00 + 0.00

Comparative quantitative study on the crystallinity of poly(tetrafluoroethylene) including Raman, infra-red and ^{19}F nuclear magnetic resonance spectroscopy

R. J. Lehnert*
Cavendish Laboratory, University of Cambridge, Cambridge CB3 0HE, UK

and P. J. Hendra
Chemistry Department, University of Southampton, Southampton SO17 1BJ, UK

and N. Everall
ICI Wilton Materials Research Centre, Middlesborough, Cleveland TS6 8JE, UK

and N. J. Clayden
School of Chemical Sciences, University of East Anglia, Norwich NR4 7TJ, UK
(Received 4 March 1996; revised 30 May 1996)

Wide-angle X-ray scattering (WAXS), ^{19}F nuclear magnetic resonance (n.m.r.) spectroscopy, differential scanning calorimetry (d.s.c.) and density measurements have been employed to determine the crystallinity of melt-quenched poly(tetrafluoroethylene) samples of different molecular weight. The methods have been checked for consistency before a routinely used infra-red (i.r.) spectroscopic and a recently devised Raman spectroscopic procedure have been correlated with crystallinity as derived by the four conventional methods. The usefulness of the two vibrational spectroscopic methods for determining crystallinity has then been assessed. It was found that WAXS, d.s.c. and density give consistent results in that they clearly show the same trends in the sample crystallinity. In contrast, neither free induction decay nor solid echo pulse sequence n.m.r. correlate with any of these methods, and possible reasons for this behaviour are discussed. Raman as well as i.r. data correlate well with the crystallinity by WAXS, d.s.c. and density. In this respect, both methods are found to be equally useful in estimating crystallinity.

(Keywords: poly(tetrafluoroethylene); crystallinity; quantitative methods including Raman and n.m.r.)

INTRODUCTION

A number of papers have appeared reporting on methods for determining crystallinity in poly(tetrafluoroethylene) (PTFE). Quantitative studies were restricted to measurements on rather small sets of samples typically consisting of less than 10 melt-crystallized specimens[1–8]. In addition, the molecular weight of the polymers used remained unspecified if the grades were characterized at all. It was, therefore, impossible to investigate whether the molecular weight has an effect on the relationship between the respective measured quantities which could be anticipated in view of an observed molecular weight dependence of the morphology[9,10]. No more than three different methods were cross-correlated in any of these studies with most of the investigations restricting themselves to a comparison of only two methods. To our knowledge no work has been published in which all conventional methods for determining crystallinity in PTFE, namely wide-angle X-ray scattering (WAXS), nuclear magnetic resonance (n.m.r.) density, differential scanning calorimetry (d.s.c.) and infra-red (i.r.) spectroscopy have been utilized to characterize the same sample set. Consequently, some doubts remained whether these methods really give consistent results. Furthermore, PTFE, upon cooling from the melt, rapidly crystallizes into a partially crystalline solid whose most prominent morphological features are thick lamellar structures. There is some evidence suggesting that the semi-crystalline material cannot be adequately described with a simple two-phase model[1,3,11,12] and more comprehensive experimental data are needed to help clarify this point. We report on a study on PTFE which was conducted with the aim of conclusively testing the aforementioned methods for consistency. Three commercial grades of different molecular weight were employed and a total of three as-polymerized and 68 melt-quenched samples were characterized to enhance the statistical significance of the correlations of the corresponding data sets. Also included in this study is a comparison of the conventional methods with a new, recently proposed procedure based on Raman spectroscopy. Although some details of

* To whom correspondence should be addressed

the latter method have already been published elsewhere[13] a comprehensive account of the procedure will be given here for completeness and also to throw some light on the nature of the exploited spectral feature. Further, the usefulness of the Raman spectroscopic method was critically assessed by comparison with its i.r. counterpart.

Crystalline PTFE exhibits three solid phases at atmospheric pressure with first-order crystal–crystal transitions occurring at 292 and 303 K, the former of which is accompanied by a relative change in density of approximately 1%[14,15]. The equilibrium melting point lies, depending on the chosen extrapolation[16], between 605 and 620 K. It is generally agreed that in the low temperature (LT) phase the molecules pack in a highly ordered triclinic structure adopting a 13/6 helical conformation having 13 equally spaced CF_2 groups in six turns. The intermediate temperature (IT) phase between 292 and 303 K is of hexagonal symmetry, the molecular helix slightly untwisting to form a 15/7 helix. The hexagonal lateral packing of the molecules is maintained in the high temperature (HT) phase, the intermolecular separation increased and the helical conformation further untwisting as the temperature is raised. It has been suggested that disorder is introduced into the crystal lattice of the IT phase by thermally activated librational motions of the chain segments and helix-reversal defects. In the HT phase, *trans* and *gauche* conformations are thought to become activated and translational motion sets in, in the chain direction disturbing the longitudinal order in the crystal lattice[14,15,17–22]. The polymeric solid is known to be highly crystalline and fully amorphous PTFE has never been observed[14,23]. Several authors have indicated that conformational, orientational and even lateral order could persist even in the molten material[23–27].

EXPERIMENTAL

Materials and sample preparation

As-polymerized commercial grade polymers were supplied in powder form by ICI, UK (Fluon G163) and Hoechst AG, Germany (Hostaflon TF1750 and KU02). According to Suwa *et al.*'s empirically derived relationship[28] between the number-average molecular weight and the heat of crystallization the molecular weight was estimated at 44×10^5, 22×10^5 and 2×10^5 g mol^{-1} for G163, TF1750 and KU02, respectively. Material that has never been melted and has been used as provided is subsequently referred to as 'virgin' polymer. The polymer powders were cold-pressed under vacuum at a pressure of 7500 kg cm^{-2} to form discs with a diameter of 13 mm and a thickness of *ca* 120 μm. The discs were heated at 650 K—well above the peak melting temperatures of the polymers—for 1 h, subsequently quenched in an ice–water bath and then annealed for various times at temperatures between 590 and 600 K to yield samples of various crystallinities. Thermogravimetric analysis confirmed that polymer degradation did not occur during quenching and annealing. X-ray diffraction (XRD) and i.r. transmission spectroscopy were applied without altering the quenched specimens. After characterization by XRD and i.r. spectroscopy, three discs, 3.6 mm in diameter, were punched out of each sample along the diameter, which coincided with the image of the diffractometer collimator slit on the sample. For the Raman measurements the three discs were stacked to increase significantly the scattering volume. Similarly, the n.m.r. measurements were made on the set of discs to improve the ^{19}F signal intensity. Subsequently, each set of discs was used to determine the density and the heat of fusion. Deviations in the measured values of the respective quantities were found to lie within the experimental error of each method for the three individual discs comprising a set. An oligomer of PTFE, n-$C_{20}F_{42}$ was obtained from Aldrich and used as provided. The melting point of the mass spectroscopy standard was measured by d.s.c. at 437 K at a scanning rate of 20 K min^{-1}.

Wide-angle X-ray scattering

Step-scan diffractograms were recorded in reflection at 298 K with a Philips 1700 diffractometer using nickel filtered Cu $K\alpha$ radiation. The data were corrected for polarization and scattering angle before deconvoluting the overlapping amorphous halo and the (100) diffraction peak[6,29]. Ratioing the integral intensities and correcting for density gives the degree of crystallinity by WAXS, X_c (X-ray). Prior to obtaining diffractograms, flat-film photographs of quenched specimens were acquired at ambient temperature to check the samples for preferred molecular orientation. Photographs were taken parallel and perpendicular to the surface plane of the specimens using forward reflection techniques and nickel filtered Cu $K\alpha$ radiation.

Nuclear magnetic resonance spectroscopy

N.m.r. measurements of crystallinity are based on associating either n.m.r. relaxation times or lineshapes found in a fit to the experimental data with the crystalline and amorphous phases within a polymer. Thus, in contrast to XRD the n.m.r. determination of crystallinity is based on the differing dynamics usually found for the crystalline and amorphous regions rather than differences in order. A fundamental assumption is that the dynamic processes characterizing the two regions have distributions largely independent of the sample. In practice this condition can be relaxed somewhat to allow for differences in the distributions providing that the effect of these variations on the n.m.r. properties still leaves the crystalline and amorphous responses distinct. The choice of the appropriate n.m.r. method is problematic. Although a linear correlation has been established between the crystallinity as found by n.m.r. multiple pulse lineshape analysis and density[2], this procedure is not suitable for a routine plant application, in view of the technically demanding character of the data acquisition.

Previous experience suggests that analysis of the free induction decay (FID) after single pulse excitation is a viable simple method for determining crystallinity[1,30,31]. Here, the fast decaying Gaussian component in the FID is identified with the crystalline phase while the slow decaying exponential is said to be the amorphous phase. Serious complications with this experiment arise in the more limited equipment suitable for plant operation because of the instrument dead times which result in the loss of the first few microseconds of data, making the initial decay of the FID very ill-defined. Solid-echo experiments overcome the problem of the instrument dead time[32] but introduce another complication, namely, the question of whether the whole of the magnetization is being refocused[33]. Complete refocusing in a solid-echo

only occurs when the dipole–dipole interaction can be treated as an isolated rigid spin-1/2 pair. Multiple spin interactions, chemical shift anisotropy and dynamic processes all introduce incomplete refocusing[34,35]. Such a case must exist in PTFE where chain dynamics are present in the amorphous phase, and although the dipole–dipole interaction in the crystalline region will be dominated by the CF_2 groupings there will also be other contributions.

Furthermore, in the crystalline region, ^{19}F spins will have a substantial chemical shift anisotropy of the order of 15 kHz. The uncertainty is then whether and to what degree back extrapolation of the fitted solid-echo components is necessary. In view of this uncertainty, back extrapolation to the start of the FID was not carried out. Providing all the PTFE samples display similar dynamic processes the only consequence of taking the fitted components from the solid-echo itself will be to introduce a proportional systematic error into the derived crystallinities.

Solid state ^{19}F n.m.r. free induction decays were measured at 188.5 MHz on a Bruker MSL200 n.m.r. spectrometer. A 5.5 μs $\pi/2$ pulse was used with a dead time of 8 μs for single pulse excitation and an interpulse delay of 8 μs for a solid-echo. In each case, 720 transients were acquired using a 5 s recycle delay, 2048 data points and a dwell time of 0.4 μs. All measurements were made in the HT phase at 333 K to emphasize the difference between the rigid crystalline and mobile amorphous T_2. The PTFE discs were left for 1 h to equilibrate at this temperature before data collection started. The FID's were then fitted to the sum of an exponential and Gaussian function using a non-linear least squares fitting method based on the Levenberg–Marquardt algorithm[36]. The mass fraction of crystalline material by n.m.r., X_c (n.m.r.), was determined by taking the ratio of the amplitude of the Gaussian signal to the total signal intensity. Experimental noise levels were found from the final 20 points of the FID.

Differential scanning calorimetry and density measurements

Absolute density measurements utilizing the sink/swim method were conducted in compliance with international standard ISO 1183 : 1987, Method C. The measurements were carried out at 296 K using 1,4-dibromobutane and dibromomethane as immersion liquids. It was verified that the effect of solvent uptake by the specimens on the measured density values stayed within the experimental uncertainty of approximately $\pm 2 \times 10^{-3}$ g cm^{-3}. Heats of fusion, ΔH_f, were determined from the melting endotherms obtained with a Perkin Elmer DSC-7 scanning calorimeter at a heating rate of 20 K min^{-1}. Values for ΔH_f were then normalized by the total weight of the semi-crystalline sample to yield the enthalpy of melting, Δh_f.

Infrared spectroscopy

I.r. transmission measurements in the range 400–4000 cm^{-1} were made on a Mattson, Galaxy 2020 spectrometer equipped with a TDGS detector. Twenty spectra with a nominal resolution of 2 cm^{-1} were co-added before processing the data, employing a method for the determination of the degree of crystallinity of PTFE proposed by Moynihan[4]. The method is based on the i.r. peak absorbances of an amorphous band at about 780 cm^{-1} and a band at 2367 cm^{-1} whose absorbance is considered to be insensitive to the molecular arrangement and hence to be only dependent on the sample thickness. According to Moynihan, the ratio A(778 cm^{-1})/A(2367 cm^{-1}) relates linearly to X_c(X-ray) and the sample density. Although our samples were some 120 μm thick they were still thin enough to allow accurate measurement of the relevant peak absorbances. Values for the absolute absorbance (peak absorbance plus baseline) at 2367 and 778 cm^{-1} lay between 0.5 and 0.7 for the former and around 1 for the latter frequency, which is within the linear range of the detector.

Raman measurements

Raman Stokes spectra with a nominal resolution of 2 cm^{-1} were recorded on a Perkin Elmer 1700X Fourier Transform Raman spectrometer equipped with an indium gallium arsenide photodetector and linearly polarized neodymium:YAG laser operating at a wavelength of 1064 nm. Scattering light of all polarization directions was collected in back-scattering geometry. Stokes shifts in the region below the Rayleigh line rejection filter cut-off at 180 cm^{-1} were inaccessible. The laser power at the sample was 500 mW, and the Norton–Beer medium apodization function[37] was chosen for Fourier transforming the interferograms, reducing the actual spectral resolution to 2.7 cm^{-1} (Rayleigh criterion). In order to improve the signal-to-noise ratio, 60 spectra were co-added. Specimens were mounted in a purpose-built sample holder equipped with a Peltier-element driven temperature stage to allow variable-temperature Raman spectra to be obtained. Spectra of crystalline and molten oligomers were recorded after a short-wave pass filter (OD$\geq$ 3 for Stokes shifts exceeding 1400 cm^{-1}) had been fitted to the spectrometer. The filter was needed to block off most of the thermal emission of the hot samples, avoiding in this way detector saturation. A conventional Dilor Raman spectrometer with 488 nm argon laser excitation was used to record spectra of molten PTFE at a resolution of about 4 cm^{-1}. Spectra of the molten polymer did not exhibit any changes over the course of 1 h, suggesting that if decomposition or any other effects occurred they caused no spectroscopic effect. All work on molten materials was conducted utilizing an aluminium sample holder fitted with a heater cartridge. None of the spectra presented here were corrected for instrument response.

RESULTS AND DISCUSSION

Primary methods: WAXS and n.m.r.

Quenched sheets of high molecular weight PTFE were reported[38] to possess a high degree of planar orientation in their surface layers. Contrary to this finding other authors[39] could not observe any preferred molecular orientation in performed and subsequently sintered samples of unspecified molecular weight. Planar orientation in which the molecular axes are parallel to the specimen surface, with a random distribution of the axes in the plane causes the equatorial reflections (*hk*0) to lie preferentially along a locus perpendicular to the surface plane, whereas (*h*0*l*) reflections tend to scatter out of the perpendicular plane. Ultimately this leads to higher relative counting rates for (*hk*0) reflections in diffractometers operating in reflection geometry. In this case, on

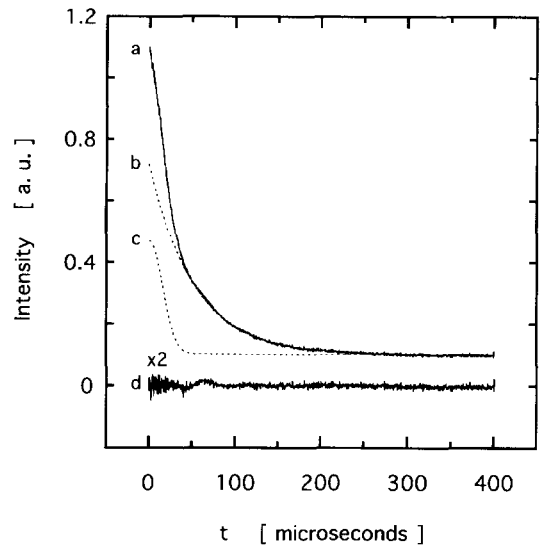

Figure 1 Typical solid-echo FID ^{19}F n.m.r. signal of melt-crystallized PTFE (solid line) and corresponding fit (a). Fitted curve is the sum of an exponential (b) and a Gaussian function (c). Curves (a)–(c) are shifted by +0.1 along ordinate for clarity. Difference (d) between measured and fitted intensity is multiplied by a factor of 2 for emphasis. Acquisition temperature was 333 K; specimen was denoted KL

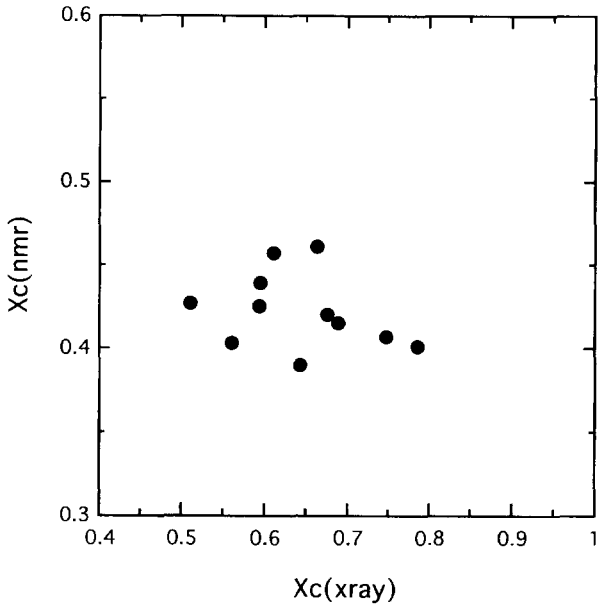

Figure 2 Mass fraction of crystalline material by solid-echo FID n.m.r., X_c(n.m.r.) *versus* the mass fraction of crystalline material by WAXS, X_c(X-ray). Filled circles = grade KU02

the assumption that amorphous material does not exhibit any type of orientation, one expects the crystallinity by WAXS to be overestimated. To check whether preferred molecular orientation plays a role here, flat-film photographs of a number of quenched specimens with widely varying heats of fusion (28–55 J g^{-1}) were taken. None of the samples made of grade KU02 exhibited any sign of preferred orientation: photographs taken from either direction showed perfect ring patterns. In contrast, all specimens made of the higher molecular weight polymers G163 and TF1750 had their diffraction rings broken into arc patterns if the photographs were taken parallel instead of normal to the specimen surface plane. All observed arc patterns, namely, of the (200), (110), (210), (107) and (108) Bragg reflections, were compatible with the samples showing planar orientation, the effect of which on the diffractograms could not be corrected. Consequently, only diffractograms of polymer KU02 could be meaningfully analysed for quantitative work. No conclusive explanation can be given here why preferred molecular orientation exclusively occurred in the higher molecular weight polymers.

All the ^{19}F n.m.r. solid-echo free induction decays could be very satisfactorily fitted to a two-phase model based on an exponential and Gaussian function. Although chemical shift oscillations might be expected to complicate the picture for the crystalline material, in practice, strong damping of the oscillations occurs as a result of the ^{19}F–^{19}F dipolar coupling, with the effect that the signal decays to zero before the first null point. The overall effect is simply to decrease T_2. A typical fit is shown in *Figure 1*. On the scale of the drawing no deviation between the fitted curve and the experimental data is apparent. Given the evidence for an oscillation in the FID, attempts were made to improve the fit using the Abragam-type function to describe the crystalline phase. However, these proved largely unsuccessful with the oscillatory term being forced to unity, reducing the Abragam function to the simpler Gaussian one. The observed time constants, T_2, are determined by the second moment of the ^{19}F–^{19}F homonuclear dipolar coupling. Values around 17 μs for the Gaussian component are typical of the crystalline phase above the 30°C phase transition while the longer exponential time constant of 70 μs reflects a reduction in the second moment from the rigid lattice value caused by the polymer dynamics. Both time constants are similar to those reported previously for PTFE[30]. A small reduction in T_2 for the Gaussian component arises as a consequence of the contribution to the dephasing from the extensive chemical shift anisotropy. On the whole, the variation in T_2 was found to be small, less than 1 μs for the Gaussian component but somewhat greater at 15 μs for the exponential component.

A plot of the crystallinity derived by n.m.r. and by XRD is shown in *Figure 2*. Overall, the correlation is poor, with the n.m.r. crystallinities covering a very limited range of values from 0.40 to 0.48, in contrast to the greater spread of those found by XRD (0.45–0.80). Having said this there is an obvious gross correlation in that both n.m.r. and XRD identify all samples as having a crystalline fraction in excess of 0.4. The failure to refocus chemical shift dephasing coupled with the finite pulse width of 5.5 μs will account for an under-reporting of the crystalline phase by a factor of the order of 0.74 based on density matrix calculation of the response of an isolated rigid CF_2 group to a solid-echo pulse sequence using the program 'Antiope'[40]. At lower magnetic fields typical of low resolution n.m.r. spectrometers used for process control this error will be negligible.

Random errors in the n.m.r. data collection and analysis procedure cannot account for either the generally low levels of crystallinity found by n.m.r. or the lack of correlation between the n.m.r. and XRD data since the repeatability of the n.m.r. crystallinity was found to be excellent (a relative standard deviation of $< 1\%$ for 20 consecutive measurements), while the reproducibility over a two-week period for eight measurements was also very good with a relative deviation of 2.5%. Perhaps the most striking example of difficulties with the n.m.r. method is the comparison

between two samples made of grade KU02, denoted KM and KL, for which the following fitted parameters were found:

$$\text{KM}: I_{exp} = 0.56,\ T_2 = 74.2\,\mu s;\ I_{gauss} = 0.46,$$
$$T_2 = 17.1\,\mu s;\ X_c(\text{X-ray}) = 0.511$$
$$\text{KL}: I_{exp} = 0.59,\ T_2 = 55.6\,\mu s;\ I_{gauss} = 0.41,$$
$$T_2 = 16.7\,\mu s;\ X_c(\text{X-ray}) = 0.748$$

The n.m.r. measurement effectively underestimates the crystallinity of KL by 0.33 while the n.m.r. and XRD values for KM are equal within experimental error. To explain this discrepancy we need to consider the possible sources of systematic errors in the n.m.r. measurements. These can be found in four areas: the n.m.r. pulse sequence, the acquisition parameters used, the fitting procedure and the two-function fit used to model the FID. Systematic errors in the pulse sequence and acquisition parameters are unlikely to cause the discrepancy seen. Errors may well result in the failure to observe all the crystalline phase, such as by incomplete refocusing of the solid-echo or poor excitation of the broad rigid phase resonance, but the nature of these errors will be to underestimate proportionately the crystalline fraction for all samples regardless of the absolute crystallinity rather than just in the case of the most crystalline samples. Only a failure of the two-phase model itself, whereby some ordered material appears to have a mobility consistent with the amorphous phase or gross changes taking place in the distribution describing the crystalline phase dynamics, will alter the n.m.r. properties sufficiently for the choice of n.m.r. experiment and acquisition parameters to be important.

Although the quality of the fitting procedure can be called into question, insofar as the fitting error is substantially greater than the experimental noise of 0.04% no amount of optimizing the fit can alter the conclusion that the short time constant fraction cannot exceed 0.5 in the case of sample KL. Statistically significant fits to n.m.r. FID data obtained for solids at high signal-to-noise ratios are very rare. In part this is a reflection of the attempt to fit a single T_2 value rather than a distribution of values, but also because the theoretical description of the expected decay is not clear when partial averaging of the dipolar interaction occurs in the presence of chemical shift oscillations. Lastly, we must not forget minor impurities, perhaps the presence of a low molecular weight oligomer, at only a level of 0.1% or so will in all probability prevent a statistically significant fit being obtained.

Having discounted systematic error in the data acquisition and analysis the only possible source of error left is the two-phase model chosen to interpret the FID. In particular the nature of the distribution describing the crystalline phase must be dependent on the individual sample. Two possible explanations for the discrepancy in crystallinity seen for KL follow from this. First, in samples of high crystallinity a substantial fraction of the crystallinity is in fact associated with regions of 'ordered' amorphous polymer which is structurally ordered PTFE with the mobile phase dynamics. Second, changes in T_2 for the mobile phase lead to an overlap in the chain dynamics, as indeed would be expected for amorphous material directly at the interface with crystalline polymer. As a consequence of the overlap in T_2 the two-function fitting leads to an artefact which can be thought of as the exponential function 'stealing' amplitude from the Gaussian function. The true explanation may well be a combination of these. Certainly, on the basis of the present work we cannot distinguish between these possibilities. Clear evidence for some change in the average dynamics of the mobile polymer is shown by all samples suspected of being highly crystalline, but reported as being low by n.m.r. For these samples we see a consistent trend of a short exponential time constant of about 55 μs. Thus, as the crystallinity of the polymer measured by XRD increases so the T_2 of the mobile phase becomes shorter. Such a reduction in T_2 would make the fitting process more susceptible to artefacts, but could also be taken to imply that the amorphous phase is taking on the characteristics of the crystalline polymer and in so doing contributes to the ordered fraction. Further confirmation of the problems associated with the two-phase model is provided by the virgin samples. Despite all being of very high crystallinity by WAXS the n.m.r. measurements consistently gave values for X_c of less than 0.5 again with a short time constant for the exponential component.

We must now consider why these problems have not been observed in previous n.m.r. studies, i.e. why highly crystalline polymer still gave a motionally averaged chemical shift lineshape. Here, the answer lies in the differing responses of the ^{19}F–^{19}F dipolar interaction being observed in the solid-echo T_2 measurements and the chemical shift tensor lineshape in the multiple-pulse experiments to the dynamic process. At all temperatures the averaging of the chemical shift tensor of the mobile component is more complete than is the averaging of the dipolar interaction; consequently, the mobile component can be more readily resolved from the rigid, crystalline component in the case of the chemical shift lineshapes. Moreover, the small changes in the amplitude of the motion with increased crystallinity observed in the T_2 measurements is unlikely to modify the chemical shift lineshape to a detrimental extent. Previous work on the ^{19}F n.m.r. FIDs has not been sufficiently extensive to deduce anything about the origin of our failure to determine high crystallinities in PTFE.

D.s.c. and density versus *primary methods*

Under the assumption of a two-phase morphological model consisting of a perfectly crystalline and a perfectly amorphous phase the mass fraction, X_c, of crystalline material by d.s.c. is given by the ratio $\Delta h_f/\Delta h_f^0$ where Δh_f^0 is the enthalpy of melting of the crystalline bulk polymer. X_c(d.s.c.) represents, regardless of the morphology, the 'equivalent mass fraction'[41] of perfect crystals which can be melted by Δh_f ignoring possible crystal–amorphous interfaces and intracrystalline defects. The actual value for X_c(d.s.c.) is, therefore, a function not only of the amount of crystalline material, but also of the crystalline perfection and the polymer morphology. To calculate X_c(d.s.c.) the enthalpy of melting of a macroscopic PTFE crystal has to be known. Values ranging from 57–104 J g^{-1} were reported in the literature (see *Table 1*) with no value appearing to be generally agreed upon. In view of this uncertainty, quoting X_c(d.s.c.) will be avoided and only the measured enthalpy of melting, Δh_f, will be used for comparison

Table 1 Literature values for the density of amorphous and crystalline PTFE, ρ_a and ρ_c at 296 K and the enthalpy of melting, Δh_f^0, of perfectly crystalline bulk PTFE

ρ_a (g cm^{-3})	ρ_c (g cm^{-3})	Δh_f^0 (J g^{-1})	Extrapolation method	Reference
2.00 ± 0.04	–	—	$1/\rho$ to X_c(X-ray) = 0 and liquid oligomers	14 18
2.060	2.302	–	$1/\rho$ to $\Delta h_f = 0$ and 93 J g^{-1}	3
2.056	2.259	—	$1/\rho$ to X_c(n.m.r) = 0 and 1	3
—	2.304 ± 0.006	—	ρ to i.r. absorbance A (778 cm^{-1}) = 0	4
—	2.30 ± 0.01	—	$1/\rho$ to X_c(X-ray) = 1	6
—	2.302	–	Crystallographic unit cell	42
—	—	93 (102)	Clapeyron equation using quenched (virgin) polymer	12
		104	Perfluoro-n-alkanes	16
—	—	57–84	Literature to 1980	12

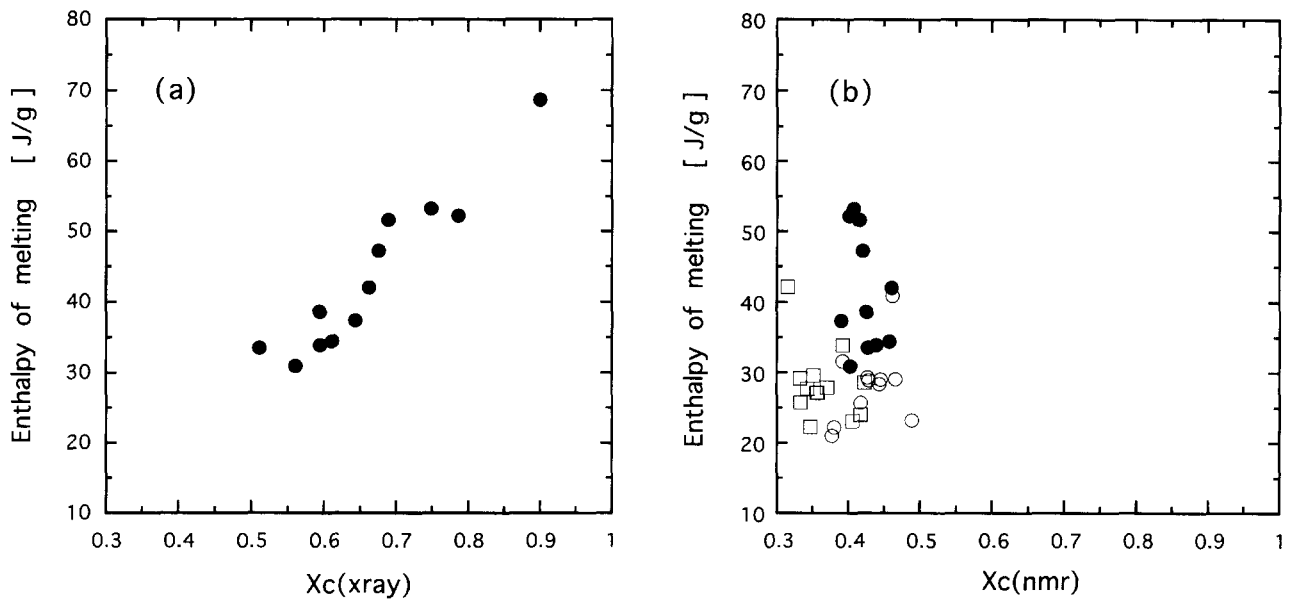

Figure 3 Enthalpy of melting *versus* the mass fraction of crystalline material by (a) WAXS and (b) n.m.r. Filled circles = grade KU02; open circles = grade TF1750; squares = grade G163

with other data sets. Due to the proportionality between X_c(d.s.c.) and Δh_f, none of the correlations will be affected by effectively setting Δh_f^0 to 1.

The measured melting enthalpies of samples of grade KU02 are plotted *versus* X_c(X-ray) in *Figure 3a*. Both quantities measure the mass fraction of crystalline material and can, therefore, be directly compared. A linear relation was assumed, an assumption that is supported by the results of a linear least-squares fit whose details can be found in *Table 2*. The extrapolated value for Δh_f^0 is roughly in the middle of the range of reported literature data and leads to a value of X_c(d.s.c.) for virgin polymer KU02 at 0.89, implying that as-polymerized PTFE is highly, but by no means fully, crystalline. A small fraction of amorphous material in virgin PTFE would agree with the observed tailing of the (100) reflection towards lower diffraction angles, which can be viewed as a weak amorphous halo merging with the Bragg peak. Extrapolation to $\Delta h_f^0 = 0$ yields X_c(X-ray) = 0.23, suggesting that a certain order could remain in the polymer even though, according to d.s.c., it would be fully amorphous. It can only be speculated whether heavily distorted crystalline material, interfacial material with some kind of structural order (although amorphous in nature for d.s.c.) or both cause d.s.c. to underestimate crystallinity in comparison with WAXS. A complete absence of correlation between the enthalpy of melting and X_c(n.m.r.) is revealed in *Figure 3b*, a finding one would intuitively expect from the comparison between WAXS and n.m.r. data in the foregoing section.

The measured density, ρ, can be used to derive the volume fraction of crystalline material, ϕ_c, according to $\phi_c = (\rho - \rho_a)/(\rho_c - \rho_a)$. As a prerequisite, the densities of amorphous and crystalline material, ρ_a and ρ_c, have to be known. *Table 1* lists literature values for these quantities as determined by the methods quoted. Obviously, ρ_a and ρ_c are not exactly known and some discrepancies persist between the different methods, giving rise to uncertainties for calculated values for ϕ_c. To avoid such uncertainties, the raw data—the measured density—and not ϕ_c will be used here for comparison with the various data sets. Since ϕ_c is a linear

Table 2 Experimental values for the density of amorphous and crystalline PTFE, ρ_a and ρ_c at 296 K and the enthalpy of melting, Δh_f^0, of perfectly crystalline bulk PTFE. Fits were linear least-squares regressions using all data points unless otherwise stated. Acronym LMW indicates that only data points of the low molecular weight grade KU02 were used for fitting. Regression coefficient is denoted R. Absolute errors indicate 67% confidence limits

ρ_a ($g\,cm^{-3}$)	ρ_c ($g\,cm^{-3}$)	Δh_f^0 ($J\,g^{-1}$)	R^2	Extrapolation method	*Figure*
—	—	77.1 ± 12.4	0.91	Δh_f to X_c(X-ray) = 1 (LMW)	*3a*
1.991 ± 0.047	2.286 ± 0.086	—	0.65	ρ to X_c(X-ray) = 0 and 1 (LMW)	*4a*
2.006 ± 0.039	2.291 ± 0.029	—	0.65	Equation (1) fitted to ρ *vs* X_c(X-ray) (LMW)	
2.074 ± 0.006	2.289 ± 0.015	—	0.87	ρ to $\Delta h_f = 0$ and 77.1 $J\,g^{-1}$	*5*
2.042 ± 0.011	2.305 ± 0.022	—	0.94	ρ to $\Delta h_f = 0$ and 77.1 $J\,g^{-1}$ (LMW)	
—	2.292 ± 0.169	—	0.90	i.r. vs ρ, abs. ratio = 0	*11a*
—	2.293 ± 0.252	—	0.92	i.r. vs ρ, abs. ratio = 0 (LMW)	
—	2.272 ± 0.182	—	0.89	Raman vs ρ, band tailing (b.t.) = 0	*11b*
—	2.271 ± 0.148	—	0.97	Raman vs ρ, b.t. = 0 (LMW)	
—	—	75.0 ± 3.4	0.90	i.r. vs Δh_f, abs. ratio = 0	*12a*
—	—	73.1 ± 5.4	0.92	i.r. vs Δh_f, abs. ratio = 0 (LMW)	
—	—	71.1 ± 6.1	0.71	Raman vs Δh_f, b.t. = 0	*12b*
—	—	66.9 ± 4.6	0.93	Raman vs Δh_f, b.t. = 0 (LMW)	

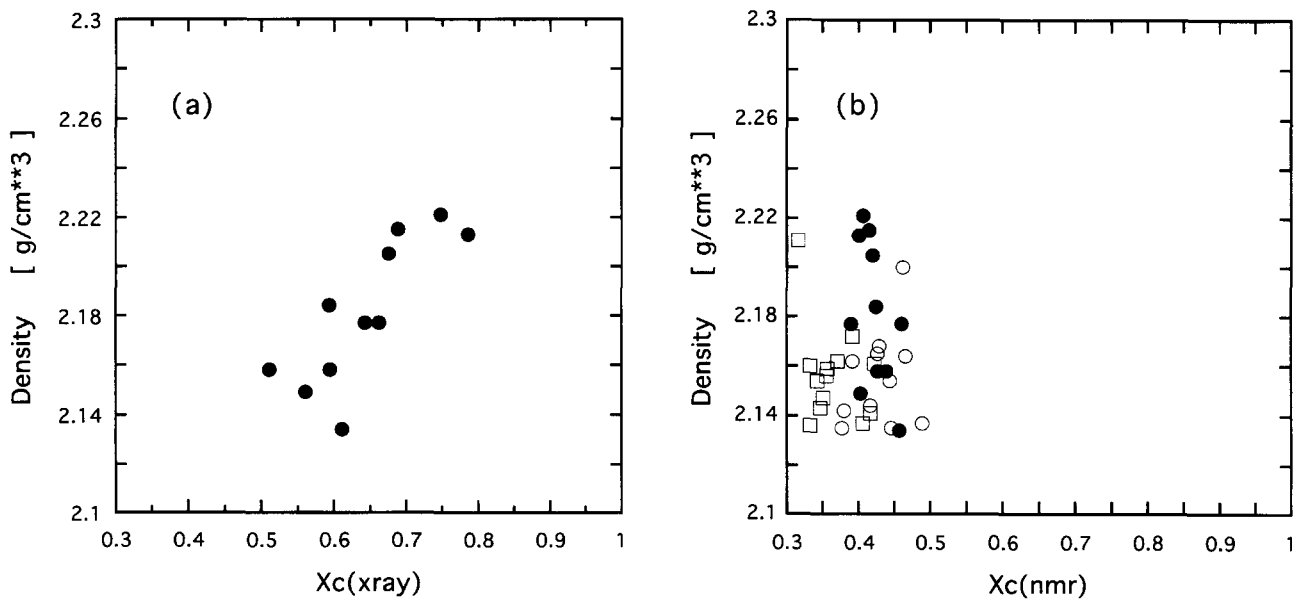

Figure 4 Density of specimens *versus* the mass fraction of crystalline material by (a) WAXS and (b) n.m.r. Filled circles = grade KU02; open circles = grade TF1750; squares = grade G163

function of ρ, a quantity which linearly correlates with ρ will also do so with ϕ_c. The crystalline volume and mass fraction are related by $\phi_c = (\rho/\rho_c)X_c$. Combining the two relations for ϕ_c and solving them for ρ , one arrives at

$$\rho = \frac{\rho_a}{1 - (1 - \frac{\rho_a}{\rho_c})X_c} \quad (1)$$

From equation (1) one would expect a non-linear relation between ρ and X_c. Assuming values for ρ_a and ρ_c of 2.0 and 2.3 $g\,cm^{-3}$ the inequality $(1 - \rho_a/\rho_c)X_c \leq 0.13$ holds and equation (1) can be simplified using simple numerical arguments:

$$\rho \approx \rho_a + \rho_a(1 - \frac{\rho_a}{\rho_c})X_c \quad (2)$$

This approximation gives the correct value for ρ at $X_c = 0$ and increasingly underestimates ρ as X_c increases. However, the approximation has a maximum deviation of −1.7% at $X_c = 1$ and can, therefore, be regarded to fit corresponding data with sufficient accuracy, justifying the use of linear regression methods in connection with ϕ_c by density. A plot of ρ *versus* X_c(X-ray) is shown in *Figure 4a*. As can be seen the data points show scatter, but clearly reveal a tendency of the density to increase as the crystallinity by WAXS increases. Linear extrapolation of X_c(X-ray) to 0 and 1 yielded values for ρ_a and ρ_c that matched the results of fits of equation (1) to the same data within less than 0.8% discrepancy while the 67% confidence limits were between 1.3 and 3.8% relative error (see *Table 2*). The derived values for ρ_a and ρ_c are, within the error limits, in good agreement with the literature values. No information on ρ_a and ρ_c could be derived from the density data as plotted against X_c(n.m.r.) that are shown in *Figure 4b*. Clearly, there is no correlation between the two quantities.

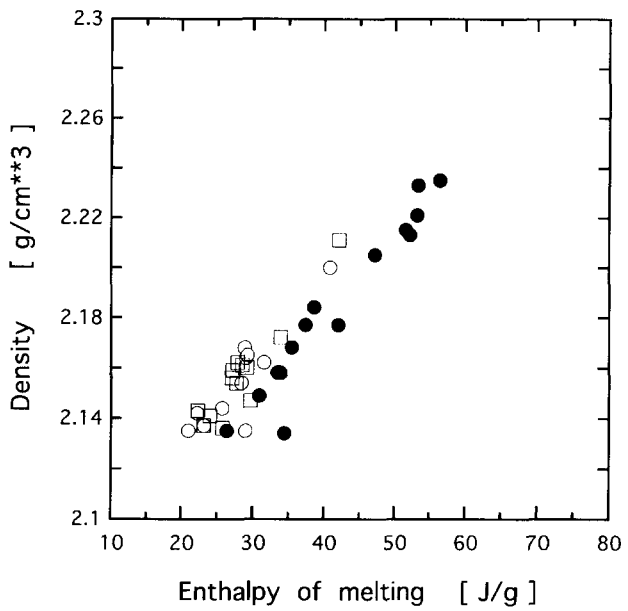

Figure 5 Density of specimens *versus* enthalpy of melting. Filled circles = grade KU02; open circles = grade TF1750; squares = grade G163

Finally, to complete the cross-correlation of the four methods the density data for all samples of the three polymer grades were compared with the enthalpy of melting. Bearing in mind what has been said above, density and d.s.c. are anticipated to depend linearly on one another. The data confirming this presumption are plotted in *Figure 5*. Linear regression analysis and curve fitting were applied to the entire data set as well as a reduced set consisting of KU02 samples only. Due to the lack of reliable literature data a value of $77.1\,J\,g^{-1}$ as determined earlier for KU02 was assumed for Δh_f^0 (*Table 2*). Fitting either equation (1) or a straight line yielded values for ρ_a and ρ_c that were equal within 0.4% deviation irrespective of whether all data points or only those of KU02 samples were used. The results of the linear fits are listed in *Table 2*. Density values as derived from the complete data set, and its KU02 subset are the same within the fitting error and are in good to excellent agreement with the literature.

Raman spectroscopic method

Several authors[8,43,44] have suggested exploitation of certain features of the Raman spectrum of PTFE for determining crystallinity. These studies were based on very few samples and were purely qualitative. Moreover, two of the studies[8,43] drew contradictory conclusions and all of them failed to explain how bulk crystallinity can actually be derived from the observed spectral changes. We have recently proposed a new Raman spectroscopic procedure for quantifying crystallinity in PTFE[13] and a brief account of the method will be given here. The proposed procedure is particularly attractive since it provides a non-destructive and exceptionally fast* means for determining crystallinity without any sample preparation requirements. In searching for an analytical principle aimed at deriving information on crystallinity from Raman spectra it is self-evident to try to decompose the Raman data into spectra of the crystalline and amorphous material. This approach did not prove feasible here because neither fully amorphous nor fully crystalline bulk PTFE has ever been observed. Attempts to subtract spectra of the melt from those of the partially crystalline solid were unsuccessful for three principal reasons. First, the high temperatures involved, let alone the melt transition itself, caused significant band broadening which could not be corrected for when subtracting the melt from the low-temperature spectrum. Secondly, the melt spectrum could not be moved as a whole along the frequency axis to make the peak positions match with those of the solid state spectra. Lastly, a spectral feature characteristic only for the melt but not the fully crystalline solid could not be identified (see Appendix, *Figure 14*). Thus, an unequivocal spectral 'standard' was missing that could suitably serve to scale the intensity of the melt spectrum prior to subtraction. Application of principal component analysis (PCA), a multivariate data analysis algorithm which allows the prediction of unknown component concentrations for multicomponent systems[45], was also unsuccessful, the main reason being that the non-linear baseline, which differed for quenched samples, could not be unambiguously subtracted prior to applying PCA.

In view of these difficulties it is clear that spectral changes had to be systematically correlated with varied sample crystallinity to identify changes that are specific and pronounced enough to prove useful for quantification. This was done in the LT phase of PTFE at 263 K, firstly in order to minimize thermally introduced inter- and intra-molecular disorder and secondly to narrow the Raman bands, thus reducing band overlap and making the distinction between different spectral features such as peaks, peak shoulders or asymmetrically broadened peak bases more obvious. Four bands, namely the ones at $\Delta\nu = 1216$, 576, 382 and $293\,cm^{-1}$, show a step-like doubling of their bandwidth between 270 and 300 K in quenched and between 280 and 300 K in virgin polymer. This sudden change in bandwidth was attributed to the onset of the solid–solid transitions and was exploited to confirm that all of the samples were indeed in the LT phase despite laser induced heating and likely temperature gradients within the specimens. Raman spectra of virgin PTFE and a sample of very low crystallinity by d.s.c. and density are shown in *Figure 6*. Line group analysis predicts 21 Raman active vibrational modes, 14 of which can be readily observed in the spectrum of virgin PTFE. There is some uncertainty about the assignments of the symmetry species to the observed Raman bands, and the reader is referred to refs 43 and 46 for details. Interest was focused on the eight strongest, and therefore potentially most suitable for quantification, Raman lines at $\Delta\nu = 1381$, 1301, 732 and $386\,cm^{-1}$ and the four bands already quoted above. All of the quoted peaks could be satisfactorily and consistently fitted with a Lorentzian model. The fitted band parameters, meaning the peak position, peak width and relative peak intensities, were then systematically correlated with the crystallinity by WAXS, n.m.r., d.s.c. and density. Correlations of relative intensities had to be restricted to adjoining peaks because diffusive elastic light scattering (all the specimens were white opaque)

* Scanning the relevant part of the Raman spectrum with a satisfactory signal-to-noise ratio can take as little as several seconds if a conventional spectrometer equipped with a CCD detector is used

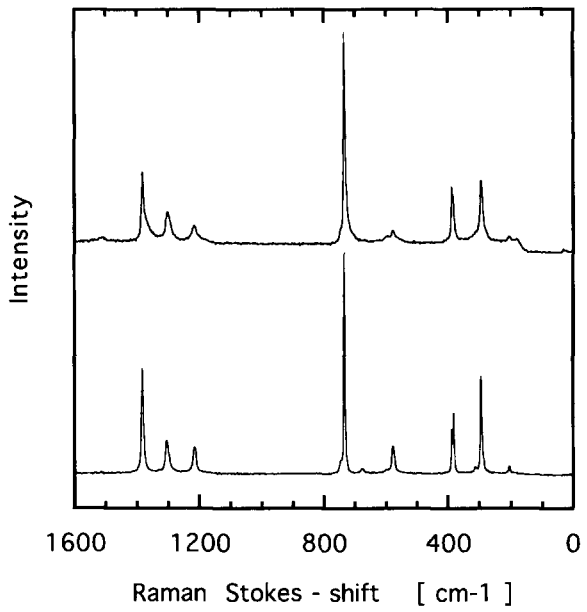

Figure 6 Raman spectra of virgin (lower curve) and quenched (upper curve) PTFE recorded at a temperature of 263 K

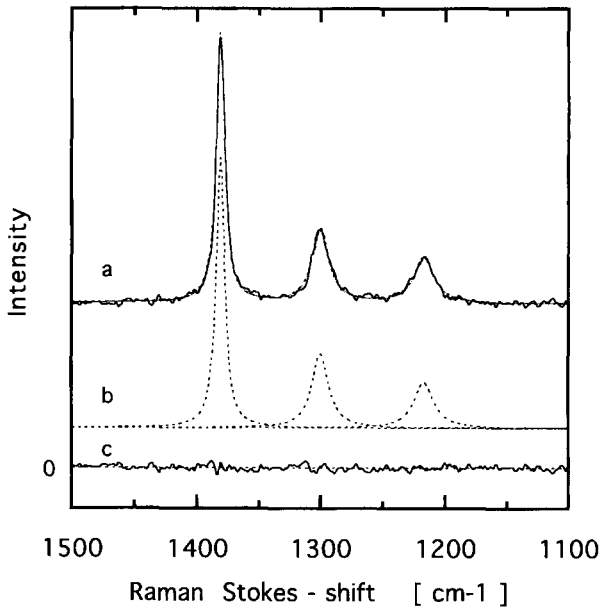

Figure 7 Relevant part of the Raman spectrum of virgin PTFE recorded at 263 K: original and fitted (dotted curve) data (a), fitted Lorentzians (b) and difference spectrum = original data–fitted data (c). Curves denoted (a) and (b) are shifted along ordinate for clarity

cause a frequency dependent attenuation of the Raman scatter. This in turn led to a strong dependence of the relative band intensity on the sample alignment, introducing a considerable error into the calculated intensity ratio if the peaks were not direct neighbours.

Shifts of band position were found to be insignificant if they exceeded the experimental error at all. The increase in bandwidth associated with the maximum decrease in crystallinity ranges, dependent on the specific mode, is from 20 to 60% of the minimal bandwidth measured for one mode. Also, the bandwidth does not always change systematically with crystallinity. Turning now to relative band intensities, either these do not change systematically with crystallinity or the changes are not pronounced enough to be useful for reliable quantification. Attention was, therefore, focused on another marked effect of decreased crystallinity, the tail forming on the low frequency side of the peak at 1381 cm^{-1}, the depolarized symmetric CF_2 stretching fundamental (see *Figure 6*). Possible causes of this tailing are discussed in the Appendix. It was found that the high frequency component of the 1381 cm^{-1} band and the complete bands at 1301 cm^{-1} (symmetric CF_2 stretching mode, depolarized) and 1216 cm^{-1} (asymmetric CF_2 stretching mode, depolarized) are almost perfectly fitted by Lorentzians. Based on this observation, the following procedure as depicted in *Figure 7* and *8* was adopted to quantify the 'band tailing'. Three Lorentzians and a straight baseline were fitted to the group of overlapping peaks in the interval between 1100 and 1500 cm^{-1}, deliberately ignoring the data between 1300 and 1380 cm^{-1}. The fitted spectrum was then subtracted from the original data, yielding a difference spectrum with non-vanishing intensities between approximately 1325 and 1375 cm^{-1}, with a maximum intensity near 1365 cm^{-1}. As the last step, the areas beneath the broad peak in the difference spectrum and the fitted Lorentzian at 1381 cm^{-1}, here denoted I(tail) and I(1381 cm^{-1}), were ratioed, giving a relative measure of the 'band tailing'.

Figure 8 shows the recorded Raman spectrum of a low crystallinity sample, the entire model spectrum fitted to these data, the Lorentzian at 1381 cm^{-1} and the difference spectrum resulting from the subtraction. Neither any additional Raman peak nor a shoulder could be resolved at liquid nitrogen temperatures. In addition, there was no indication of the difference spectrum changing its shape and overall appearance with temperature and crystallinity apart from a slight broadening as the temperature rose. The ratio of integrated intensities R, defined as quotient I(tail)/I(1381 cm^{-1}) can be reliably determined and is reproducible within a statistical error or around 4%. The value R is not affected by the solid–solid phase transitions and stays almost constant between 173 and 395 K except for a slight decrease as the temperature is raised, which can be explained with an increasing overlap of the Raman fundamental with its 'tail' due to band broadening. A word of warning appears appropriate here: the actually measured values for R are, rather unsurprisingly, affected by the chosen spectral resolution, $d\nu$, and it was experimentally established that R decays exponentially with $d\nu$. This can be understood again in the light of a Raman peak and its asymmetric base that merge to an increasing extent and, therefore, become progressively indistinguishable as the spectral resolution deteriorates. From a certain value for the resolution onwards the 'tail' will become completely obscured by the Raman peak eventually leading to $R = 0$. However, it could be confirmed that R falls with the same rate for samples with very different crystallinity, hence ensuring that correlations of R with other quantities do not become a function of $d\nu$.

I.r. and Raman versus *primary methods, density and d.s.c.*

To find out whether the vibrational spectroscopic methods devised in ref. 4 and in the preceding section can add another means for determining crystallinity or not,

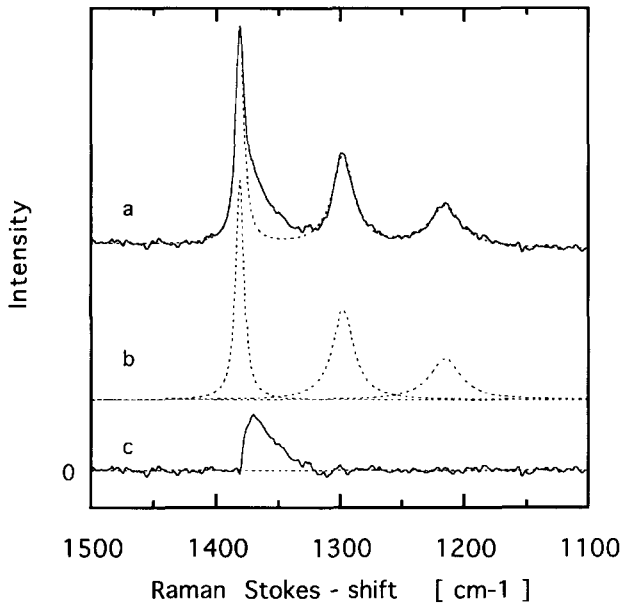

Figure 8 Relevant part of the Raman spectrum of quenched PTFE recorded at 263 K: original and fitted (dotted curve) data (a), fitted Lorentzians (b) and difference spectrum as described in the text (c). Curves denoted (a) and (b) are shifted along ordinate for clarity

i.r. and Raman data were compared with the already cross-correlated methods, three of which were found to give consistent indications of crystallinity. Including the i.r. method by Moyniham[4] in this comparison was considered necessary particularly in view of findings[47] which called the crystallinity independence of the i.r. 'thickness' band at 2367 cm^{-1} into question. Another reason for cross-checking the i.r. method was that ref. 4, in fact, provided indirect evidence only for its claim of excellent correlation of the absorbance ratio with X_c(X-ray). The i.r. absorbance ratio is plotted *versus* X_c(X-ray), X_c(n.m.r.), ρ and Δh_f in *Figures 9–12*, respectively. As can be seen in *Figure 9a* the plotted data clearly support a linear relationship between the absorbance ratio and X_c(X-ray), but the data points are somewhat scattered indicating that X_c(X-ray) correlates to i.r. within an uncertainty of some ±10% rather than ±1% as claimed by Moynihan[4]. The regression line extrapolates at X_c(X-ray) = 0.98 ± 0.17 for a vanishing absorbance ratio independent of whether virgin polymer (single data point at $X_c = 0.9$) was disregarded or not. *Figure 10a* reveals, in accordance with the corresponding plots of ρ and Δh_f against X_c(n.m.r.), no significant correlation between the i.r. data and the crystallinity by n.m.r.

Comparison of the i.r. data with ρ and Δh_f in *Figures 11a* and *12a*, in turn, undoubtedly reveals that either quantity is linearly related to the absorbance ratio, but again the data are scattered to a certain extent. The extrapolated values for ρ_c and Δh_f^0 are, although more affected by scatter and therefore less accurate, in good agreement with the results obtained earlier (see *Table 2*).

Plots of the quantified 'band tailing' R *versus* X_c(X-ray), X_c(n.m.r.), the density and the enthalpy of melting are depicted in *Figures 9b–12b*, respectively. Without doubt R correlates linearly with all quantities other than X_c(n.m.r.) for the low molecular weight polymer KU02. The statistical significance of the latter two correlations, expressed as the squared regression coefficient, falls by 10–20% if in addition the two higher molecular weight polymers are included (see *Table 2*). The correlation with density data is relatively unaffected by the molecular weight compared with the calorimetric data as can be seen in *Figures 11b* and *12b*, in the latter of which data points of samples of different polymers appear to lie on different straight lines. Increasing scatter occurs for the polymer G163 as Δh_f decreases. We presume that a molecular weight dependence of the morphology could be the underlying cause. A transmission electron microscopy study by Suwa *et al.*[10] suggests that melt-crystallized PTFE forms lamellar or fibrillar structures for polymers with molecular weights above 10^6 g mol^{-1} and below 3×10^5 g mol^{-1}, respectively. According to Suwa *et al.*, disordered inter- and intralamellar material composed of molecules with highly irregular conformations causes the lamellar morphology

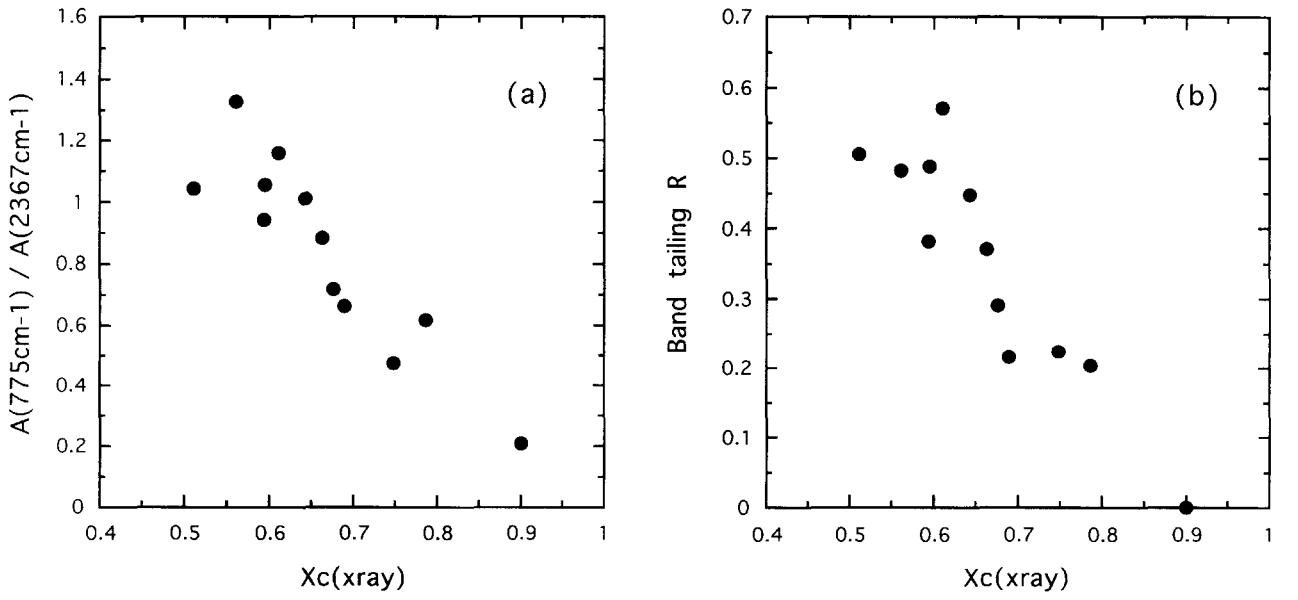

Figure 9 I.r. absorbance ratio (a) and 'band tailing' R as defined in the text (b) *versus* the mass fraction of crystalline material by WAXS. Filled circles = grade KU02

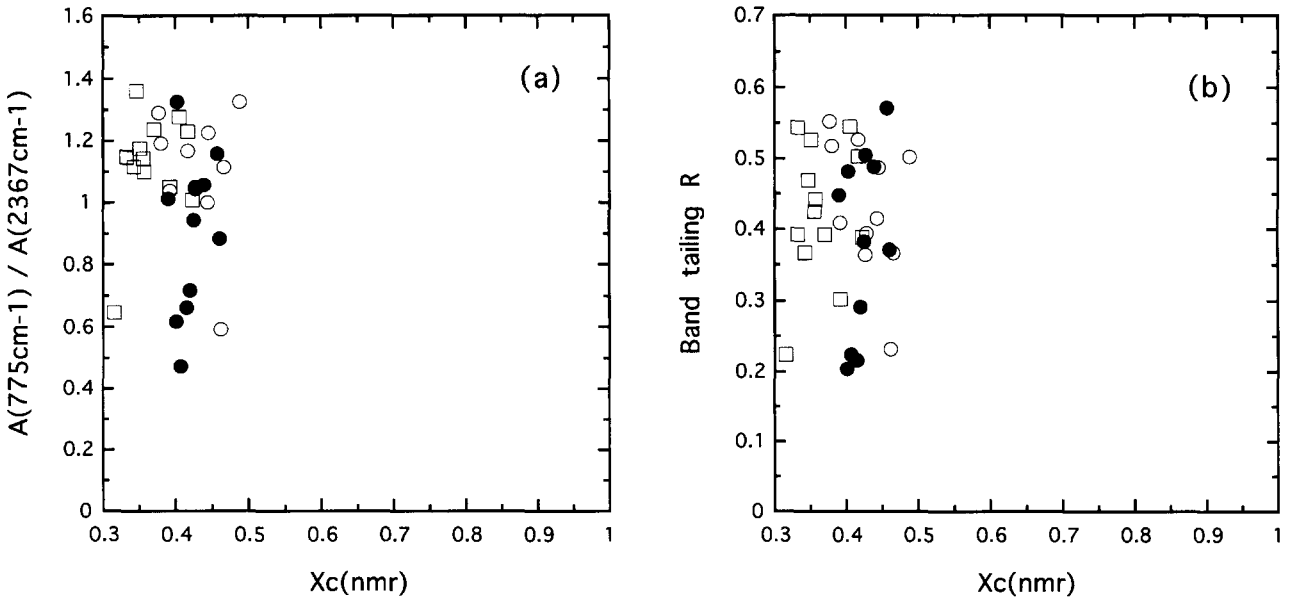

Figure 10 I.r. absorbance ratio (a) and 'band tailing' R as defined in the text (b) *versus* the mass fraction of crystalline material by n.m.r. Filled circles = grade KU02; open circles = grade TF1750; squares = grade G163

to be less ordered than is the case for the fibrillar one. Polarizing light micrographs of 2 μm thick strips microtomed from samples examined in this study also hint at different morphologies. All micrographs showed irregularly distributed dot-like or dash-shaped birefringent regions with the latter exclusively appearing in polymer KU02. Another distinct difference between the low and the two high molecular weight grades is that micrographs of the former always revealed very evenly distributed birefringent regions whereas crystalline regions in the other grades tended to agglomerate and form comparatively compact 'clouds' in an otherwise amorphous matrix. Evidently, such morphological differences could be expected to influence the correlations, but it remains unclear why quantities other than Δh_f seem little affected if at all.

Turning now to the results of linear regression analysis carried out on the data sets, R extrapolates to zero at X_c (X-ray) = 0.91 ± 0.16 whether virgin polymer is included or not, which compares reasonably well with the value of 0.98 from i.r. data. The values for Δh_f^0 as extrapolated from the entire sample set and samples made of KU02 only were different with the latter being significantly lower. This finding indicates that certain dissimilarities between low and high molecular weight PTFE exist, but their cause remains unknown. However, with the corresponding results from i.r. measurements and the correlation of d.s.c. data with X_c(X-ray) one arrives at the conclusion that Δh_f^0 for melt-crystallized polymer lies somewhere between 70 and 75 J g^{-1}. Using the values for Δh_f^0 from Raman and i.r. to extrapolate to ρ_c in *Figure 5* one obtains a crystalline density of 2.272

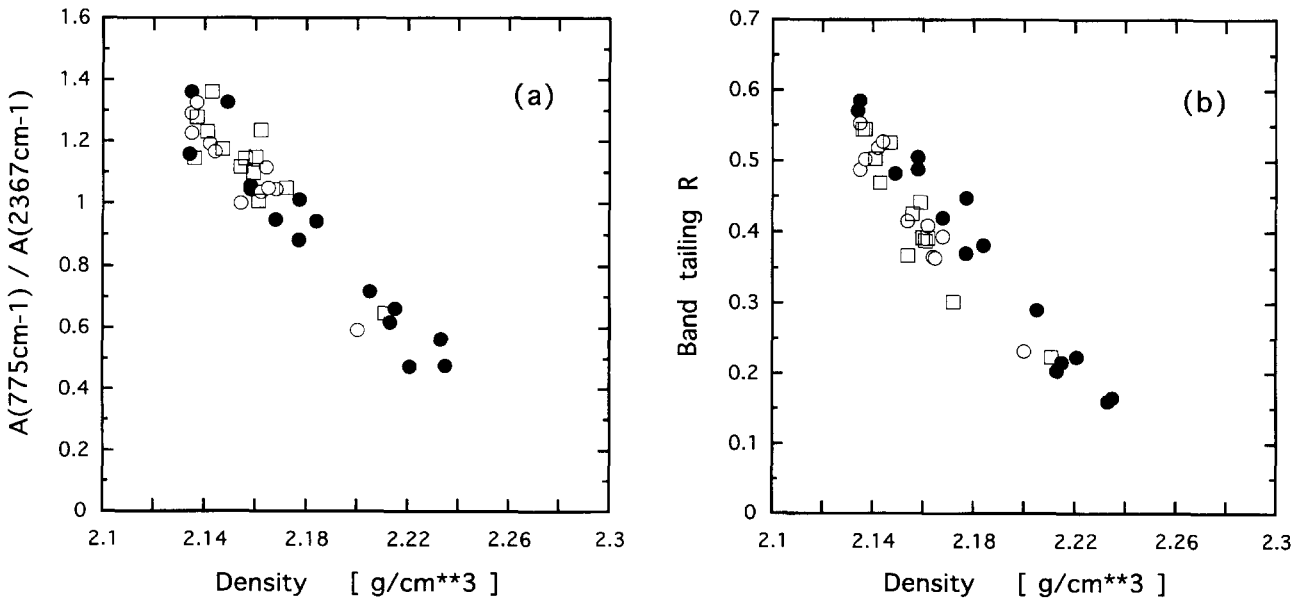

Figure 11 I.r. absorbance ratio (a) and 'band tailing' R as defined in the text (b) *versus* the density of the specimens. Filled circles = grade KU02; open circles = grade TF1750; squares = grade G163

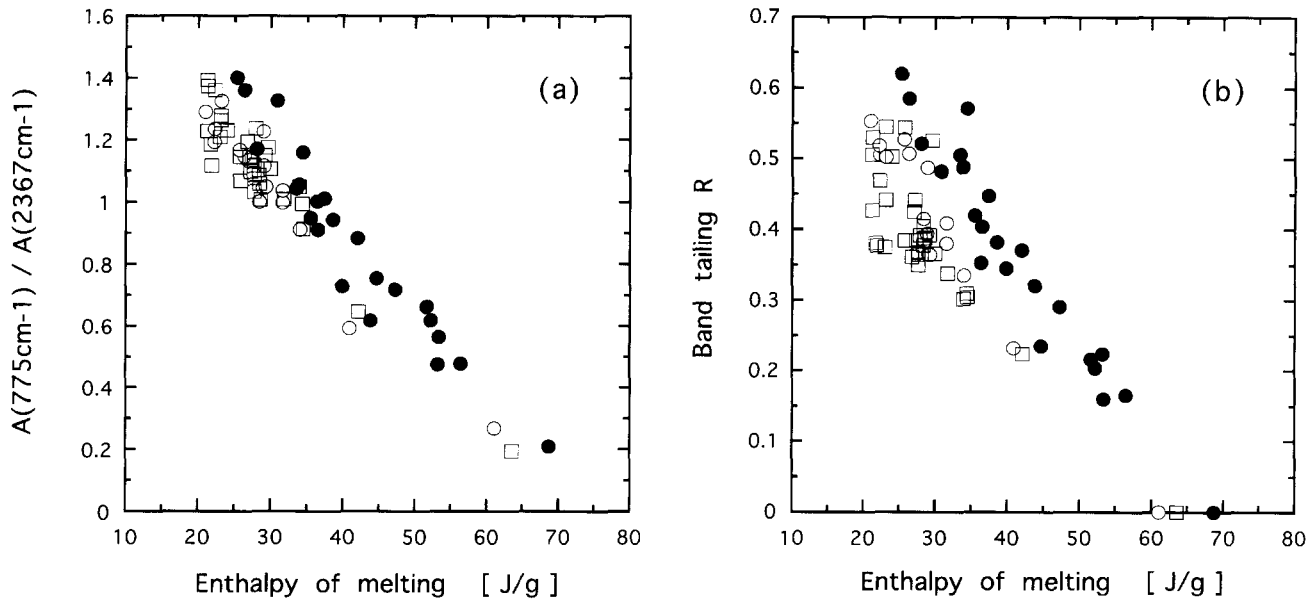

Figure 12 I.r. absorbance ratio (a) and 'band tailing' R as defined in the text (b) *versus* the enthalpy of melting. Filled circles = grade KU02; open circles = grade TF1750; squares = grade G163

(2.270) and 2.283 (2.291) $g\,cm^{-3}$ if all (only KU02) samples are used for fitting. These figures are significant to within approximately $\pm 0.020\,g\,cm^{-3}$. Finally, extrapolation of R to zero in *Figure 11a* yields a value for ρ_c that is independent of whether only grade KU02 was considered or not. A compilation of the extrapolation results can be found in *Table 2*.

All of the values for ρ_c and Δh_f^0 determined here agree well with the literature data. It is worth noting that the value of ρ_c of $2.272\,g\,cm^{-3}$ is rather low and closest to the one of $2.259\,g\,cm^{-3}$ derived from n.m.r. measurements[3]. In ref. 3 it is presumed that the discrepancy between $2.259\,g\,cm^{-3}$ and the crystallographic density of $2.302\,g\,cm^{-3}$ may reflect properties of interfacial material between crystalline and amorphous regions. If this interfacial material has the density

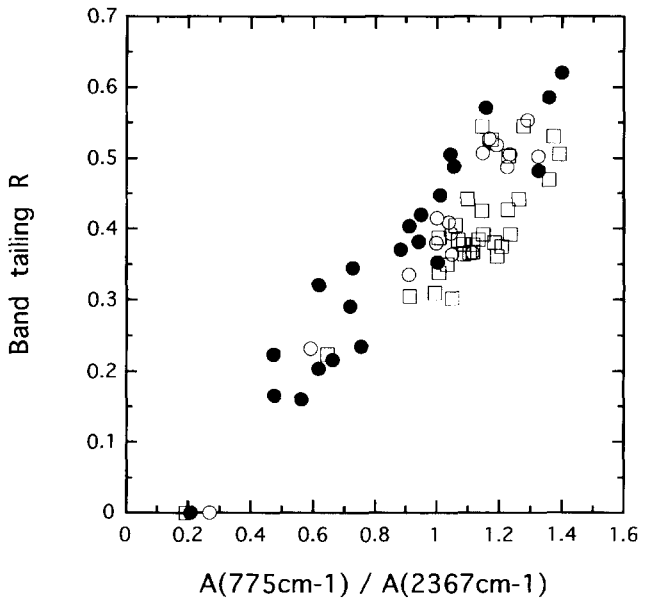

Figure 13 'Band tailing' R as defined in the text *versus* the ratio of i.r. absorbances. Filled circles = grade KU02; open circles = grade TF1750; squares = grade G163

of the amorphous phase, but not its mobility as seen by n.m.r. extrapolation to $X_c(\text{n.m.r.}) = 0$ would give consistent results with other methods, but extrapolation to $X_c(\text{n.m.r.}) = 1$ would not and, indeed, in the same study the density ρ_a was in excellent agreement with methods other than n.m.r. It may be speculated that the intensity ratio R exclusively measures the amount of structurally 'truly' amorphous material while Δh_f is a measure of a, in the same sense, 'true' crystalline phase, and both methods are insensitive to a presumed third component of intermediate order. If one assumes that KU02 forms only two phases during crystallization whereas the other two grades are able to form a third at the expense of a 'true' crystalline phase it could then be explained why R relates linearly to Δh_f for the former polymer and why the 'band tailing' deviates towards lower values for the other grades as the crystallinity by d.s.c. decreases. Raman would measure the same amount of amorphous material for a low and higher molecular weight specimen, but the latter would have, due to the intermediate phase, a smaller crystalline content by d.s.c. The scatter which severely affects the data could be due to varying amounts of the intermediate phase as quenching and subsequent annealing cannot always be expected to result in the same distribution of the originally molten material between the three phases. From the smaller deviation between the different grades at higher values for Δh_f one could further presume that the amount of material in an intermediate state of order, if existent at all, decreases as the amorphous fraction becomes smaller.

Eventually, to complete the set of possible cross-correlations, R is plotted against the i.r. absorbance ratio in *Figure 13*. The data were found to be unaffected by the molecular weight and they undoubtedly support the view of a linear relationship between both quantities. The absorbance ratio extrapolates at -0.045 ± 0.026 for $R = 0$ and the squared regression coefficient equals 0.81. Ignoring the data points of virgin polymer one arrives at values of -0.006 ± 0.033 and 0.71 for the same parameters.

From what has been said it may be stated with care that the Raman and i.r. spectroscopic methods are

similarly sensitive to the amount of amorphous material present in the sample.

CONCLUSIONS

WAXS, d.s.c. and density measurements were found to give consistent results in that they clearly show the same trends in sample crystallinity while the derived values for the degree of crystallinity are comparable, but not identical. Each method correlates linearly with the respective two other methods, which was shown here for the first time for the same set of samples. Quenched specimens with a molecular weight larger than $2 \times 10^6\,g\,mol^{-1}$ exhibited planar orientation and for this reason had to be excluded from the WAXS data, limiting the meaningfulness of the cross-correlation to a certain extent. Comparisons of ^{19}F solid-echo FID n.m.r. with either of the aforementioned three methods did not reveal a significant degree of correlation and the crystallinity by n.m.r. appeared to be generally lower than by WAXS. Causes for this discrepancy, which is not observed in multiple-pulse n.m.r., were considered and an explanation is given on the basis of a failure of the assumed two-phase model. However, there is a possibility that the polymer dynamics are not unequivocally related to regions that are either amorphous or crystalline by WAXS and that, for instance, material which is crystalline by X-ray may exhibit dynamics more akin to amorphous polymer. Since the data on the samples are insufficient in this respect it cannot be decided here which explanation is the more probable one. The increasing 'tailing' of the Raman band at $\Delta\nu = 1381\,cm^{-1}$ was identified as a pronounced spectroscopic effect arising from decreased crystallinity. Several possible causes for this phenomenon were discussed, but its origin remains unclear. A procedure for quantifying the 'band tailing' was devised and comparison with WAXS, d.s.c. and density showed that the corresponding quantity can serve as a measure for the crystallinity. Correlations of the i.r. method by Moynihan[4] with WAXS, d.s.c. and density have equal statistical significance compared with the Raman procedure. Both methods were, in this respect, found to be equally useful in estimating crystallinity. The molecular weight had an effect on the correlation of the 'band tailing' with d.s.c., which is thought to be due to a molecular weight dependence of the sample morphology. The observed deviation in the Raman *versus* d.s.c. plots can be tentatively explained if one assumes that a morphological two-phase model for melt-crystallised PTFE is insufficient for higher molecular weight polymer. All methods employed here were found to estimate rather than accurately measure crystallinity in PTFE.

ACKNOWLEDGEMENTS

The provision of polymer samples by Hoechst AG, Gendorf, Germany, and ICI 'Fluon', Hillhouse, UK, is gratefully acknowledged. ICI are also thanked for financial assistance. R.J.L. further wishes to thank F. Kestler for financial support.

REFERENCES

1 Iwayanagi, S. and Sakurai, I. *J. Polym. Sci.: Part C* 1966, **14,** 29
2 Vega, A. J. and English, A. D. *Macromolecules* 1980, **13,** 1635
3 Starkweather, H. W. *J. Polym. Sci.: Polym. Phys. Edn.* 1982, **20,** 2159
4 Moyniham, R. E. *J. Am. Chem. Soc.* 1959, **81,** 1045
5 Pyereligin, I. S., Peskova, M. Z., Zakirov, Z. Z. and Glinkin, I. M. *Zh. Prikl. Spektrosk. (USSR)* 1976, **24,** 1027
6 Ryland, A. L. *J. Chem. Educ.* 1958, **35,** 80
7 Hu, T.-Y. *Wear* 1982, **82,** 369
8 Rabolt, J. F. *J. Polym. Sci.: Polym. Phys. Edn.* 1983, **21,** 1797
9 Seguchi, T., Suwa, T., Tamura, N. and Takehisa, M. *J. Polym. Sci.: Polym. Phys. Edn,* 1974, **12,** 2567
10 Suwa, T., Seguchi, T., Takehisa, M. and Machi, S. *J. Polym. Sci.: Polym. Phys. Edn.* 1975, **13,** 2183
11 Villani, V., Pucciariello, R. and Ajroldi, G. *J. Polm. Sci., Part B: Polym. Phys.* 1991, **29,** 1255
12 Starkweather, H. W., Zoller, P., Jones, G. A. and Vega, A. J. *J. Polym. Sci.: Polym. Phys. Edn.* 1982, **20,** 751
13 Lehnert, R. J., Hendra, P. J. and Everall, N. *Polymer* 1995, **36,** 2473
14 Brandrup, J. and Immergut, E. H. (Eds) 'Polymer Handbook', Vol. 29, 2nd Edn, John Wiley, New York, 1975
15 Tadakoro, H. 'Structure of Crystalline Polymers', John Wiley, New York, 1989, pp. 15, 157 and 354
16 Starkweather, H. W. *Macromolecules* 1986, **19,** 1131
17 Bunn, C. W. and Howells, E. R. *Nature* 1954, **18,** 549
18 Sperati, C. A. and Starkweather, H. W. 'Fortschritte der Hochpolymeren-Forschung (Advances in Polymer Science)' (Eds J. D. Ferry and C. G. Overberger), Vol. 2, Springer Verlag, Heidelberg, 1961, p. 465
19 Yamamoto, T. and Hara, T. *Polymer* 1982, **23,** 521
20 Weeks, J. J., Sanchez, I. C., Eby, R. K. and Poser, C. I. *Polymer* 1980, **21,** 325
21 Weeks, J. J., Eby, R. K. and Clark, E. S. Polymer 1981, **22,** 1496
22 Kilian, H. G. *Kolloid Z. Z. Polym.* 1962, **185,** 13
23 Sherratt, S. 'Kirk-Othmer Encyclopedia of Chemical Technology', 2nd Edn, Interscience, New York, 1966, pp. 805–831
24 Toneilli, A. E. *Polymer* 1976, **17,** 695
25 Khanna, Y. P., Chomyn, G., Kumar, R., Murthy, N. S., O'Brian, K. P. and Reimschuessel, A. C. *Macromolecules* 1990, **23,** 2488
26 Rosi-Schwartz, B. and Mitchell, G. R. *Polymer* 1994, **35,** 3139
27 Lovell, R., Mitchell, G. R. and Windle, A. H. *Farad. Disc. R. Soc. Chem.* 1980, **68,** 46
28 Suwa, T., Takehisa, M. and Machi, S. *J. Appl. Polym. Sci.* 1973, **17,** 3253
29 Kilian, H. G. and Jenckel, E. *Z. Elektrochem.* 1959, **63,** 308
30 McCall, D. W., Douglass, D. C. and Falcone, D. R. *J. Phys. Chem.* 1967, **4,** 998
31 Wilson, C. W. and Pake, G. E. *J. Chem. Phys.* 1957, **27,** 115
32 Powles, J. G. and Strange, J. H. *Proc. Phys. Soc (London)* 1963, **82,** 6
33 Mansfield, P. *Phys. Rev.* 1965, **137,** A961
34 Boden, N., Levine, Y. K. and Squires, R. T. *Chem. Phys. Lett.* 1974, **28,** 523
35 Boden, N., Levine, Y. K., Lightowlers, D. and Squires, R. T. *Mol. Phys.* 1975, **29,** 1877
36 Press, W. H., Flannery, B. P., Teukolsky, S. A. and Vetterling, W. T. 'Numerical Recipes: The Art of Scientific Computing', Cambridge University Press, Cambridge, UK, 1986
37 Norton, R. H. and Beer, R. *J. Opt. Soc. Am.* 1976, **66,** 259
38 Clark, E. S., and Starkweather, H. W. *J. Appl. Polym. Sci.* 1962, **6,** S41
39 Marega, C. and Marigo, A. *Makromol. Chem.* 1989, **190,** 1425
40 Debouregas, F. S. and Waugh, J. S. *J. Magn. Reson.* 1992, **96,** 280
41 Chen, H.-L. and Hwang, J. C. *Polymer* 1995, **36,** 4355
42 Clarke, E. S. and Muus, L. T. *Z. Kristallogr.* 1962, **117,** 108
43 Peacock, C. J., Hendra, P. J., Willis, H. A. and Cudby, M. E. A. *J. Chem. Soc. (A)* 1970, **18,** 2943
44 Willis, H. A., Cudby, M. E. A., Changry, G. W., Nicol, E. A. and Fleming, J. W. *Polymer* 1975, **16,** 74
45 Haarland, D. M., Easterling, R. G. and Vopicka, D. A. *Appl. Spectrosc.* 1985, **39,** 73
46 Bower, D. I. and Maddams, W. F. in 'The Vibrational Spectroscopy of Polymers' (Eds R. W. Cahn, E. A. Davis and I. M. Ward), Cambridge University Press, Cambridge, UK, 1989, p. 185
47 Starkweather, H. W., Ferguson, R. C., Chase, D. B. and Minor, J. M. *Macromolecules* 1985, **18,** 1684
48 Schwickert, H., Strobl, G. and Kimmig, M. *J. Chem. Phys.* 1991, **95,** 280
49 Rabolt, J. F. and Fanconi, B. *Polymer* 1977, **18,** 1258

APPENDIX

To aid in elucidating the origin of the tailing' of symmetric CF_2 stretching band at 1381 cm^{-1} several possible causes for this phenomenon will be discussed below. Subsequently quoted fundamental modes, corresponding symmetry species and frequencies are compiled in ref. 46.

'Hot' bands

The prerequisite for the occurrence of 'hot' bands is the thermal excitation of vibrational states above the ground state. Consequently, the intensity of 'hot' bands will fall as the temperature is reduced. Here, the energy difference between the ground state and the first excited state was measured at $\Delta E_{0,1} \approx 170$ meV corresponding to 1380 cm^{-1}. Since the intensity, $I_{n,n+1}$ of a Raman band is proportional to the population of the initial state involved in the transition the relative intensity of a 'hot' band ($I_{1,2}/I_{0,1}$) is proportional to $\exp(-\Delta E_{0,1}/kT)$ with the usual notation. Hence, reducing the temperature from 370 to 170 K should result in a drop of the relative intensity by a factor of approximately 500. Here, it was found that the intensity ratio R stays nearly constant between 170 and 370 K and it can, therefore, be reliably concluded that the 'band tailing' is not caused by the phenomenon of 'hot' bands. Another argument against the occurrence of 'hot' bands is that even the first excited vibrational level would not be sufficiently populated at temperatures below $T = \Delta E_{0,1}/k \approx 2000$ K to contribute to any significant extent to the Raman intensity.

Overtone bands

The weak Raman-active band at 676 cm^{-1} (E_2 symmetry species) would be the most likely candidate for an overtone close to but below 1352 cm^{-1} = 2 × (676 cm^{-1}) which would be within the range of the 'band tailing' (1325 to 1375 cm^{-1}), but below the frequency of the peak in the difference spectrum at 1365 cm^{-1}. The overtone would have a component with A_1 symmetry, which is Raman active. However, without assuming that Fermi resonance takes place, it could not be understood how this weak band can give rise to a fairly strong (R can reach values up to 0.7) peak that overlaps with the fundamental at 1381 cm^{-1} (A_1). This fundamental could enhance the intensity of the overtone, but would at the same time be expected to change at least slightly both its intensity and position, which was not observed. In addition, the fundamental at 676 cm^{-1} considerably weakens in low crystallinity specimens where the band 'tailing' is most pronounced (*Figure 6*). In view of this evidence and having discounted second and higher order harmonics the possibility that an overtone causes the 'band tailing' was ruled out.

Combination bands

Three bands would prove suitable as combination bands in terms of their sum frequency:

(1) 102 (?), m + 1242 (E_1), vvs = 1344 cm^{-1}
(2) 203 (E_1), s + 1152 (E_1), vvs = 1355 cm^{-1} ($A_1 + A_2 + E_2$) (3 symmetry species refer to 1355 cm^{-1} band)
(3) 638 (A_2), s + 732 (A_1), vvs = 1370 cm^{-1} (A_2)

Combination band (3) can be excluded on the grounds that a band with A_2 symmetry would be i.r. active but Raman silent. The remaining two bands should both be i.r. active because a combination of a fundamental belonging to any of the four possible symmetry species with 1242 cm^{-1} band results in an i.r.-active mode. The i.r. transmission spectra of virgin and quenched PTFE were carefully examined, but no indication was found of bands occurring in the relevant frequency range. Although this absence of i.r. bands does not necessarily imply that the above combination bands do not exist it seems improbable that a combination band is the underlying cause of the 'band tailing'.

Relaxation of selection rules

The factor group mode at 1381 cm^{-1} corresponds to a vibrational mode with phase difference $\delta = 0$ between adjacent CF_2 units. As a consequence, the position of the mode on the dispersion curve is fixed and, therefore, the band frequency cannot be affected by a change of the helix pitch unless the force constants are also changed. On the other hand, it seems likely that the molecule can develop variability of its helix pitch in disordered material, which would destroy the translational symmetry along the chain. This, in turn, would remove the basis of a description through line group methods. The same holds for strongly curved stretches of the molecule such as loops or entanglements. In either case, factor group analytical arguments could not be expected to apply rigorously and modes with a phase angle $0 \leq \delta \leq \Delta\delta$ may be spectroscopically active. If one assumes that the approximate dispersion curves in ref. 46 are correct, one would expect the band at 1381 cm^{-1} to broaden asymmetrically as observed and to exhibit, in this respect, the most marked effect of the Raman bands investigated here. The asymmetric broadening could be explained in this way, but since the molecular conformation in the quenched material and the manner in which it might affect the spectroscopic selection rules are unknown no further conclusions are drawn.

Inhomogeneous broadening

It is quite instructive to look at the spectra of molten PTFE, which can be reasonably presumed to be the most disordered phase. *Figure A1* shows three Raman spectra of the same sample of virgin PTFE, which was slowly heated to temperatures above the melting point at about 620 K. The similarity between the spectra is striking. In fact, the melt spectrum appears, in terms of the number of modes and the peak pattern, to be identical with the spectrum of the solid polymer, and from the accessible frequency range (50–2000 cm^{-1}) it is concluded that the spectroscopic selection rules for Raman activity do not break down upon melting. Therefore, a considerable degree of molecular symmetry is maintained in the melt. This presumption is in agreement with neutron diffraction[26] and WAXS[27] studies on molten PTFE where it was proposed that PTFE molecules are more or less straight for some 25 Å (20 carbon atoms) and that straight chain segments are likely to pack locally in a parallel manner. 'Tailing' of the Raman line in question was observed from about 595 K onwards and was found to become stronger up to the melting temperature. The temperature at which 'band tailing' sets in coincides well with the onset of the melting endotherm between 590 and 600 K at a heating rate of 20 K min^{-1}. Apparently, the melting process and the accompanying increase in

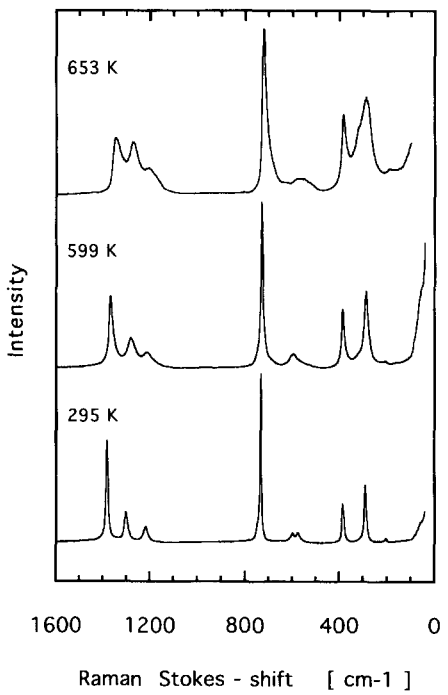

Figure A1 Raman spectra of virgin PTFE at three different temperatures on heating above the melting point at approximately 610 K. Spectra were recorded using a conventional Dilor Raman spectrometer with 488 nm excitation

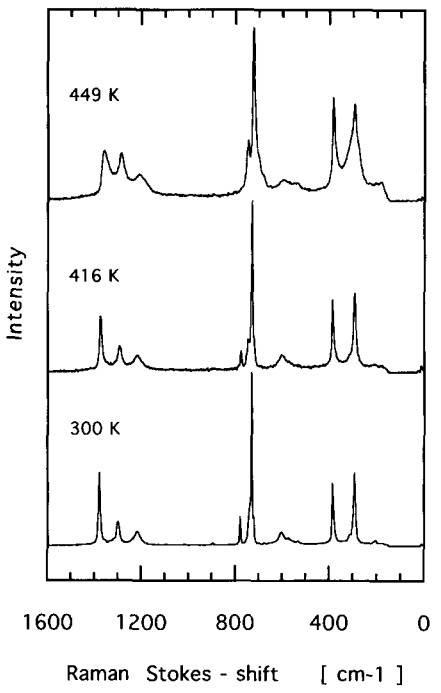

Figure A2 Raman spectra of n-$C_{20}F_{42}$ at three different temperatures on heating above the melting point of 437 K. Spectra were recorded using a *FT* near i.r. Raman spectrometer equipped with a short-wave pass filter; excitation wavelength was 1064 nm. Background at 449 K was caused by thermal emission of sample

disorder play a vital role here and it is suggested that the molecular conformation in amorphous regions of quenched material is similar to the one in the melt. A corresponding series of Raman spectra of the oligomer n-$C_{20}F_{42}$ is shown in *Figure A2*. n-$C_{20}F_{42}$ is known to have a 15/7 helical conformation[48] above 200 K, like PTFE above 292 K, and to possess a regular conformation over some 12 backbone atoms in the melt[49]. The spectra of the oligomer and the polymer are virtually identical in most respects apart from two progression bands at 780 and 900 cm^{-1}. Also, they seem to be equally affected by the melt transition. There is one distinct difference, though, the 1381 cm^{-1} band in the oligomer is slightly asymmetric in the melt, but clear signs of 'tailing' as observed in the polymer were missing when the data were fitted. Obviously, both the polymer and the oligomer exhibit some degree of conformational order in the melt, but the oligomer would on a microscopic scale lack conformational features such as entanglements and loops which are normally assumed to be present in molten polymers. With care it may be hypothesized that the 'band tailing' is caused by sequences of CF_2 units with irregular conformations that are located in entanglements, chainfolds or polymer specific conformational defects. Notwithstanding what has been said above this hypothesis is somewhat speculative and, in particular, it does not explain why broadening occurs exclusively on the low frequency side of the peak. It appears that this argument makes it more probable that the cause for the observed phenomenon can be linked to a relaxation of the Raman spectroscopic selection rules rather than inhomogeneous broadening.